KSME

Springer

Journal of Mechanical Science and Technology 36 (5) 2022

Original Article
DOI 10.1007/s12206-022-0432-z

Keywords:
· Carbon fiber reinforced polymer
· Cutting tool temperature
· Edge trimming
· Tungsten carbide cutter
· Tool life
· Tool wear

Correspondence to:
Deviprakash Jyothi Devan
djyothi@okstate.edu

Citation:
Devan, D. J., Almaskari, F., Sheikh-Ahmad, J., Hafeez, F. (2022). A study on tool wear of tungsten carbide cutters in edge trimming of CFRP. Journal of Mechanical Science and Technology 36 (5) (2022) 2499~2510.
http://doi.org/10.1007/s12206-022-0432-z

Received May 19th, 2021
Revised January 3rd, 2022
Accepted January 6th, 2022

† Recommended by Editor Hyung Wook Park

A study on tool wear of tungsten carbide cutters in edge trimming of CFRP

Deviprakash Jyothi Devan[1,2], Fahad Almaskari[1], Jamal Sheikh-Ahmad[1] and Farrukh Hafeez[1,3]

[1]Department of Mechanical Engineering, Khalifa University of Science and Technology, Abu Dhabi, United Arab Emirates, [2]School of Mechanical and Aerospace Engineering, Oklahoma State University, Stillwater, OK 74078, USA, [3]DIAC, University of Birmingham Dubai, Dubai, United Arab Emirates

Abstract Carbon fiber reinforced polymer (CFRP) composites are widely used in the aerospace field because of their outstanding lightweight material characteristics, tensile strength, and stiffness properties. The tools used in composite machining exhibits different cutting performance and machining quality under different cutting conditions. The combination of tool material, tool geometry, and cutting conditions strongly influence the tool life and surface quality of the machined parts. Edge trimming of CFRP blanks with tungsten carbide two flute end mill cutter was conducted. The operation was carried out on a computer numerical control (CNC) router by varying cutting speed, feed speed, and depth of cut. Experimental results indicated that the wear of carbide tools is characterized by abrasive wear and rounding of the cutting edge. This occurred mainly by hard abrasion of the carbide grains. Tool life was observed to be inversely proportional to cutting speed, feed speed, and depth of cut. An expanded tool wear equation with power, average temperature, and resultant force as independent variables provided higher tool wear predictive capabilities. To check the adequacy of the regression model, validation runs were conducted. The experimental tool wear obtained from validation experiments were compared with the tool wear obtained using regression. An approximate average error of 5 % confirms that the experimental and regression tool wear values are very close. The equations and analysis permit trimming of CFRP to be designed such that tool wear is optimized and well forecasted.

1. Introduction

Machining of composite materials, especially during secondary stages like edge trimming, drilling, and grinding, differs from machining homogenous materials as the properties of composites are heavily reliant on fiber type, fiber direction, and matrix present [1]. Studies suggest that composite machining involves a series of uncontrolled fractures along with very small plastic deformation [2, 3]. Consequently, tools used for the machining of composites are subjected to continuous thermal and fatigue stresses and alternating cutting forces, which may lead to abrasive tool wear, chipping, clogging of the flutes, and chip notching [4, 5].

The failure of the tool happens when it fails to produce parts with dimensional accuracy and required surface finish. This makes tool wear an important benchmark in the selection of tool materials. Tool wear is regarded as the removal of the material from the surface of a tool due to the combined effects of various physical and chemical processes. The studies in the calculation of tool wear are not conclusive due to the complexity of the problem and relatively higher dependence on experiments. Moreover, these tests are time-consuming and expensive [6].

Tool wear is characterized by the removal of hard particles from the tool surface due to abrasion, vibration, or impact at the workpiece-tool interface [7]. It is a gradual process and is the result of the cumulative effect of different mechanisms like erosive wear, diffusion wear, corrosive wear, oxidation wear, and fracture. The proportion of these mechanisms on total tool wear depends on the cutting forces, feed speed, cutting speed, and temperature [8, 9]. Tool wear can facilitate delamination and burn, leading to increased tool forces and temperature at the ma-

chined surface [10]. Different authors have concluded that tool wear, cutting forces, and cutting temperature are greatly dependent on feed speed, cutting speed, and depth of cut [11-16].

One of the most common types of tools used in the machining of CFRP is tungsten carbide cutters. Tungsten carbide tool is conventionally used in the edge trimming of CFRP and produces clean cut even at higher feed speeds. The wear mechanism in tungsten carbide tools while machining CFRP can be best described by cobalt extrusion and micro abrasion [17, 18]. Initially, the cumulative effect of plastic deformation and soft abrasion removes the cobalt from the tungsten carbide grains. This, in turn, weakens the tungsten carbide bond facilitating the removal of carbide grains. Furthermore, the cutting edge of the tool suffers from severe rounding while machining CFRP [19]. This is due to the epoxy matrix, which has viscoelastic properties. Moreover, tool wear has a notable effect on surface roughness, temperature, force, and power, although their relative dependence varies [20-22].

Studies conducted by Davim and Reis [23] concluded that surface roughness increases with the feed speed and decreases with cutting speed. By using a cutting speed of 110 m/min and a feed speed of 0.04 mm/rev, they were able to achieve a surface roughness of 1.02 μm on composites using a cemented carbide end mill. However, investigations by Haddad et al. [20] with tungsten carbide and diamond coated burr tools on CFRP suggest that such a correlation exists only at standard cutting conditions. At higher cutting conditions, surface roughness is primarily dependent on cutting speed and not on feed speed.

To study the influence of temperature on cutting conditions, Takeshi and Takayuki [24] used an infra-red camera based dynamic temperature response system to measure the tool-workpiece temperature in the milling of CFRP using a cemented carbide end mill cutter. They noted that the temperature saturates at higher cutting speeds between 100 m/min to 300 m/min. Studies with carbide tools at constant speed confirmed that an increase in feed speed could lead to an increase in cutting temperature [11]. This was confirmed by Weinert and Kempmann [25], whereas Chen reported the contrary [26].

To study the influence of force on cutting conditions, Janardhan [27] conducted routing of CFRP with tungsten carbide tools of 6.35 mm diameter. He studied the normal force, feed force, and axial force along x, y, and z directions, respectively, and observed that these parameters increase with an increase in cutting distance. Using six flute carbide tools on CFRP, Slamani [28] observed that when a cutting tool gets worn, more force is needed to remove the material. He reported that there is an exponential increase in cutting forces with an increase in cutting length. Koplev et al. [12] suggested that cutting force is proportional to the depth of cut. Ucar and Wang [15] conducted trimming of CFRP using a helical end mill cutter and stated that cutting forces increase with feed speed and decrease with cutting speed. The cutting force in a coated tool is low compared to an uncoated one due to the low coefficient of friction at the tool chip interface of a coated tool [21]. It is also noticed that the cutting forces developed during the machining of CFRP undergoes fluctuation. The anisotropic nature of CFRP is the major reason for this nonlinear change of cutting force [29]. Studies also revealed that net power increases with cutting distance, feed speed, and tool wear [27].

The existing literature covers both the qualitative and quantitative aspects of tool wear and the factors influencing it. However, the studies in the calculation of tool wear of tungsten carbide tool in edge trimming of CFRP are not conclusive due to the complexity of the problem and dependence on experiments. A clear understanding of the optimum cutting conditions combining tool wear with cutting parameters (feed speed, cutting speed, and depth of cut) and response variables (surface roughness, temperature, force, and power) has not yet been developed. The current study aims at developing a tool wear equation that would reveal the effect of both cutting parameters and response variables and how these correlates with tool wear. The investigation provides theoretical and quantitative guidance to related research works in the comparison of the performance of different tools with respect to service life and quality of the work piece.

2. Experimental procedure

Experimental work was conducted in the Composites Lab of Khalifa University, Abu Dhabi. CFRP panels of the dimension of 500 mm × 500 mm × 10 mm and TiN coated tungsten carbide tools were used in the study. Fig. 1 and Table 1 show the specimen and specifications of the CFRP. The tungsten carbide tool and its specifications are shown in Fig. 2 and Table 2, respectively.

Table 1. Specifications of CFRP.

Feature	Description
Material type	Carbon fiber fabric/epoxy resin
Fiber	Carbon
Matrix	Epoxy
Fabric	Balanced weave, twill 2×2
Mode of manufacture	Autoclave molding
Curing temperature	180 °C
Resin content	42 %
Glass transition temperature	150 °C

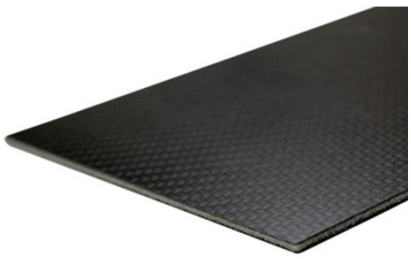

Fig. 1. CFRP specimen used in the study.

Table 2. Specifications of tungsten carbide tool.

Feature	Description
Name	Tungsten carbide end mill cutter
Make	SGS
Code	SER 03S-48641
Diameter	10 mm
Coating	TiN
Cutting tolerance	± 0.05 mm
Body	Tungsten carbide
Number of cutting edge	2
Length of cutter	75 mm
Length of cutting edge	22 mm
Helix angle	30°

Fig. 2. Tungsten carbide tool used in the research.

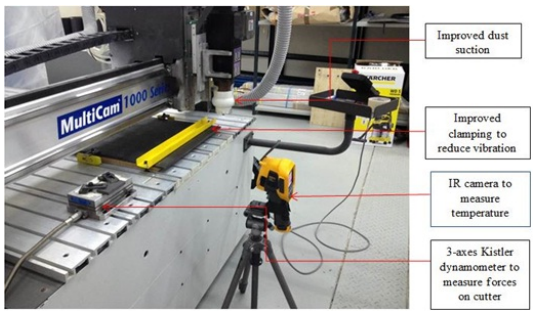

Fig. 3. CNC router used in the machining operation and the cutting set up.

The CFRP specimens were subjected to edge trimming using a three-axis MultiCam CNC router (Fig. 3). The measurements taken during machining include temperature, force, and power (Fig. 4). The temperature of the workpiece- tool interface was measured using a Fluke Ti400 infra-red (IR) camera. The camera was set so that it gave an instant in-focus image of the cutting region every three seconds. The IR images thus obtained were analyzed using SmartView software. Cutting force measurement during the machining operation was recorded using a tri-axis piezoelectric dynamometer (Kistler Type 9272). The forces that were studied during the trimming operation were the normal force along the x-direction (F_x), feed force along the y-direction (F_y), and axial force along the z-direction (F_z). Root mean square (RMS) was used to represent force with a single value, referred hereby as resultant force. A universal power cell was used to measure the real power given to the spindle motor during machining. The net cutting power (P) at the end of each pass was determined as the difference between the total spindle power and the idle power (i.e., spindle turning without cutting).

A full factorial design, 2^n was used in this study as shown in

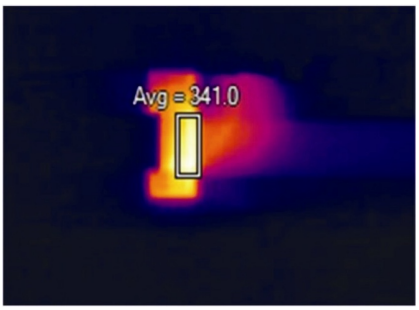

(a)

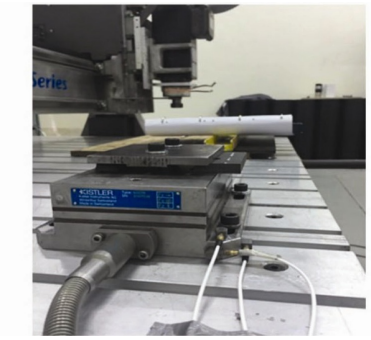

(b)

(c)

Fig. 4. (a) IR image under analysis using SmartView; (b) dynamometer setup; (c) power cell set up.

Table 3. The cutting parameters comprising the three independent variables, namely feed speed, cutting speed, and depth of cut, have two levels: high (+), low (-). In total, there are eight cutting combinations (Table 4). They are named R1, R2, R3, R4, R5, R6, R7, and R8 for simplicity in later discussions [30]. The ranges of the cutting parameters were selected based on the suggested values provided by the tool manufacturer. Emissivity value used for the tool was 0.29.

Each combination of feed speed, cutting speed, and depth of cut was repeated two times, and the two readings were averaged. The post-process stage of measurement includes the determination of surface roughness, tool wear, and microstructure. The surface roughness of the blanks was measured using surface roughness tester Mitutoyo SJ-301 (Fig. 5). The measurements were conducted on five distinct locations on the machined edge, and the two roughness parameters, arithmetical mean roughness value (R_a) and mean roughness depth (R_z),

Table 3. Milling factors and levels for tungsten carbide tool.

Factors	Level	Value	Level	Value
Cutting speed (V)	+	6400 rpm	-	4000 rpm
Feed speed (f)	+	1000 mm/min	-	500 mm/min
Depth of cut (d)	+	5 mm	-	2.5 mm

Table 4. Factorial design of experiment for tungsten carbide tools.

Test	f	V	d
R1	-	-	-
R2	-	+	-
R3	+	-	-
R4	+	+	-
R5	-	-	+
R6	-	+	+
R7	+	-	+
R8	+	+	+

Fig. 5. Surface roughness tester.

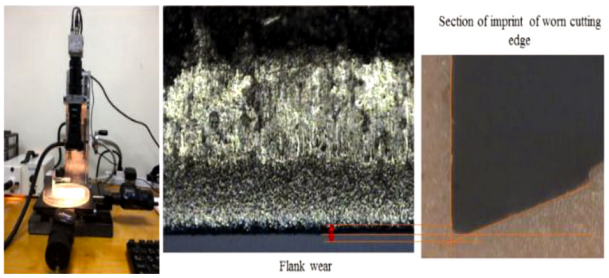

Fig. 6. Setup of the optical microscope with the tool holding fixture and the flank wear at the tool edge.

were measured for each location. Measurement of flank wear was conducted after every pass using an optical microscope (Fig. 6). To quantify tool wear, flank wear was measured. Maximum flank wear corresponds to the maximum width of the wear land on the clearance face. The flank wear is the average of the two flank wear readings recorded for each flute. Using Sigma scan pro image analysis software, the measurements of tool wear and analysis of image was done. The microstructure of the worn tool was analyzed using a scanning electron microscope (FEI-Quanta 250 ESEM).

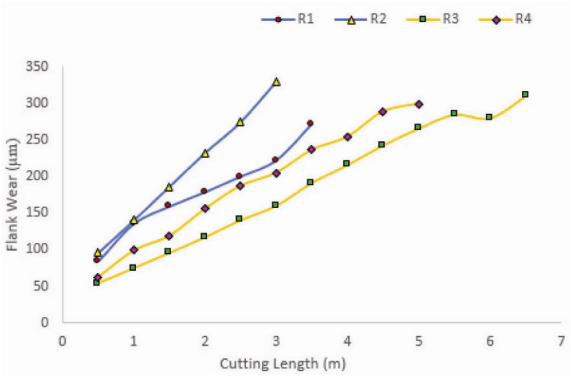

(a)

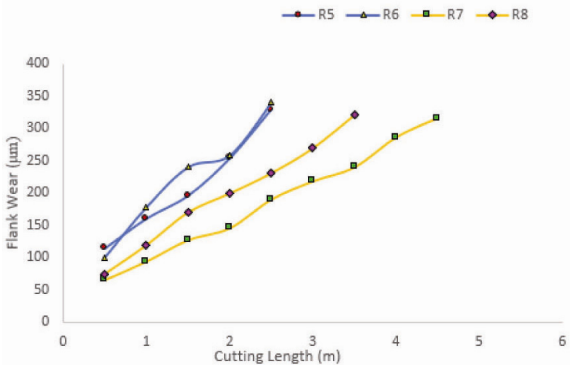

(b)

Fig. 7. Variation of flank wear against cutting length: (a) of R 1, 2, 3, 4; (b) of R 5, 6, 7, 8.

3. Results and discussions

3.1 Tool wear

Flank wear was studied for approximately 300 µm. The variation of flank wear was plotted against cutting length for different cutting conditions, as shown in Fig. 7. After every 0.5 m of trimming distance, the tool was removed to inspect the cutter flutes under the optical microscope to determine the magnitude of tool wear. Based on the tool wear curve, the tool life equation was developed using nonlinear regression for a cutting length corresponding to 200 µm flank wear as follows.

$$T = 2.24543\, V^{-0.58473} f^{-0.23991} d^{-0.56209}. \quad (1)$$

To check the adequacy of the tool life equation, the main effect plot and interaction plot was generated using Minitab software (Fig. 8). The similarity in the plots of single and two-factor interaction confirms that the tool life of carbide tools is inversely proportional to feed speed, cutting speed, and depth of cut. Fig. 9 highlights the interactions of different parameters on tool life. It can be noted that the products of the depth of cut with feed speed and cutting speed are the key interactions.

From Fig. 9(a) it can be noted that there is a steep increase in flank wear with the cutting length. This should be due to the severe chipping and delamination of the TiN coating. It was

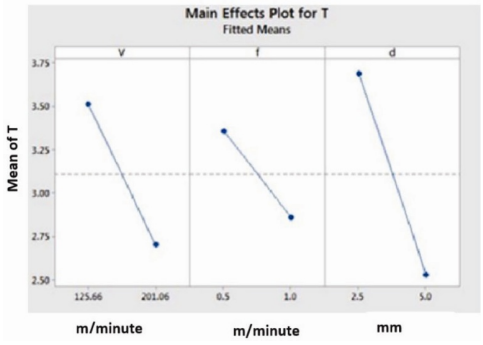

(a)

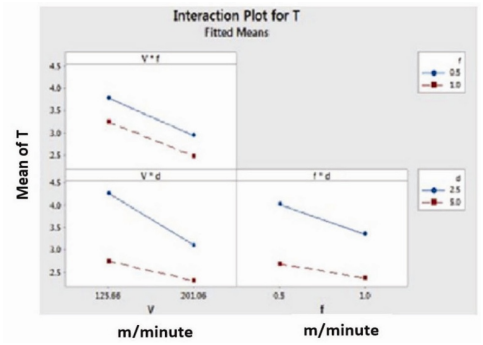

(b)

Fig. 8. Effect of feed speed, cutting speed, length of cut and depth of cut on tool life: (a) main effect plot; (b) interaction plot.

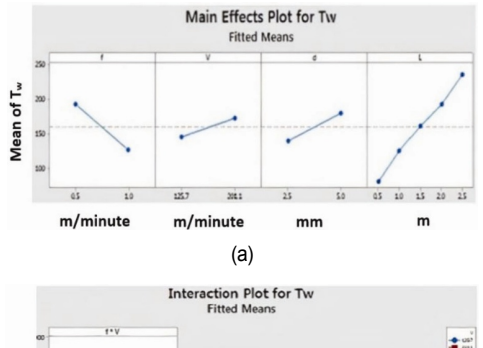

(a)

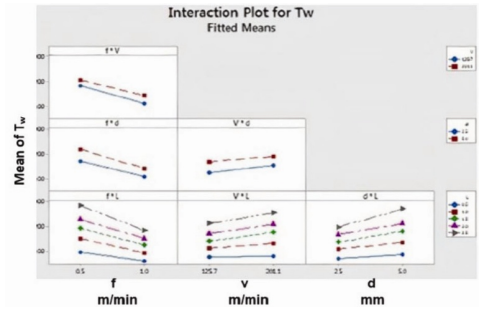

(b)

Fig. 9. Effect of feed speed, cutting speed, length of cut and depth of cut on tool wear: (a) main effect plot; (b) interaction plot.

also noted that as cutting length increased, resins and fibers got adhered to the cutting edges. The literature proposes that after this abrupt increase in tool wear, the wear progresses slowly. This secondary stage of wear is attributed to the abrasion of the coating and substrate. However, this region is absent in the current research as the cutting length is confined to a value corresponding to approximately 300 μm flank wear.

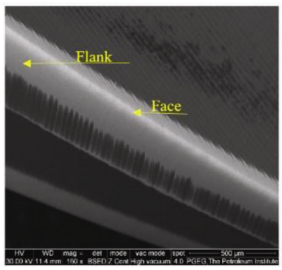

(a)

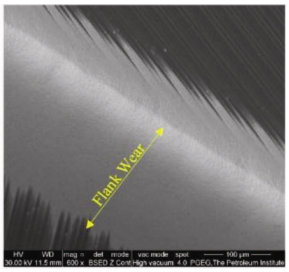

(b)

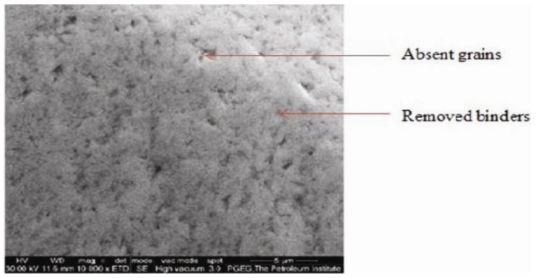

(c)

Fig. 10. (a), (b), (c) show the SEM images of the wear pattern of carb ide tools under cutting condition R3 at magnifications 160x, 600x and 10000x, respectively.

3.2 Tool wear mechanism

The wear of carbide tools was attributed to abrasive wear and rounding of the cutting edge. Figs. 10(a)-(c) show the SEM images of the wear pattern of carbide tools under cutting condition R3 at magnifications 160x, 600x, and 10000x, respectively. The SEM image (a) and (b) show the flank wear and degree of roundness of the cutting edge. The wear develops by the removal of the cobalt binder present between the carbide grains followed by the removal of carbide grains by fracture initiating crack formation. The SEM image (c) shows the voids and intergranular cracks formed when carbide grains are removed. The black dots in the image are the cobalt binder that was removed during hard abrasion, revealing the carbide grain. The high values of cutting forces could be the reason for the binder to partially extruded from the tool.

3.3 Surface roughness

It can be observed that R_a decreases with an increase in cutting speed. This is evident from the R_a-cutting length curves (Fig. 11) by comparing the cutting conditions R1 with R2 and R5 with R6, which demonstrates the effect of cutting speed. R1 and R5 are low cutting speed conditions, while R2 and R6 are high-speed ones. The tool, when used under the cutting condition R1 and R5, showed higher values of R_a relative to R2 and R6, respectively. However, when feed speed is increased, the

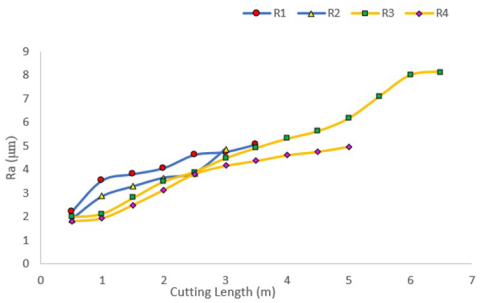

(a)

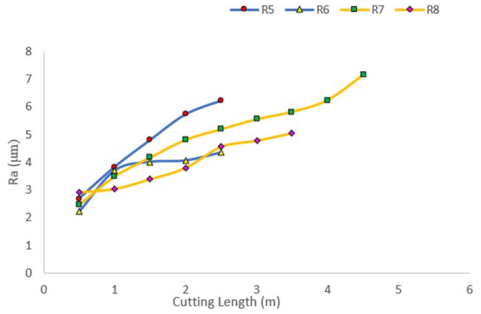

(b)

Fig. 11. Variation of R_a against cutting length: (a) of R 1, 2, 3, 4; (b) of R 5, 6, 7, 8.

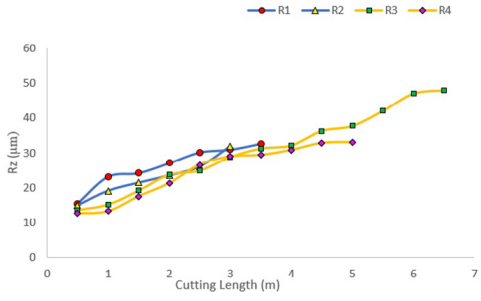

(a)

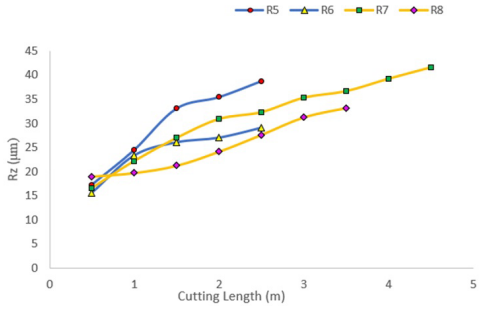

(b)

Fig. 12. Variation of R_z against cutting length: (a) of R 1, 2, 3, 4; (b) of R 5, 6, 7, 8.

value of R_a also increased. R1 and R5 are low feed conditions, while R3 and R7 are high feed ones. The increase in R_a with higher feed speed is obvious by comparing R1 with R3 and R5 with R7. Hence, it is clear that surface roughness parameters are inversely proportional to cutting speed and directly proportional to feed speed and depth of cut. At low cutting speeds, large material removal is noticed, leading to higher surface roughness. An increase in cutting speed can cause a decrease in chip per tooth and less deformed matrix and fibers leading to a lower R_a. On the other hand, an increase in feed speed can cause increased heat generation, higher chip thickness, and chatter leading to incomplete machining of the workpiece and consequently higher roughness. This was evident during the experiment as visible cracks were present on the surface when machined under the cutting conditions R3 and R7 [31]. It was also noted that at higher cutting lengths, surface roughness showed a steep increase in all the cutting conditions. It can be inferred that R_z is more sensitive to surface roughness than R_a. The trends discussed for R_a is also applicable to R_z (Fig. 12).

3.4 Temperature

The average and maximum temperatures of the cutting tool were found to be directly proportional to cutting length and cutting speed but inversely proportional to feed speed. This is confirmed by the SEM images and wear measurements, which reveal the deterioration of the sharp tip of the tool, facilitating wear and rubbing friction, consequently increasing the temperature. Figs. 13 and 14 explain the variation of average and maximum temperatures with respect to cutting length.

A large portion of heat from the tool is lost into the chips. The decrease in average and maximum temperature with higher feed speed is obvious by comparing R1 with R3 and R5 with R7. In the course of thermography, it was noted that at high feed conditions like R3 and R7, the chip temperature was higher, which justifies the argument.

The dependence of feed rate on temperature can be explained on the basis of material removal rate. Decrease in temperature with higher feed speed is due to the high material removal rates. It has been shown in recent studies that the heat partition in machining CFRP consists of heat conducted to the tool, heat conducted to the workpiece and the remaining heat evacuated by the chips. The latter partition is the largest. Therefore, increasing the feed results in increasing the chip thickness and thus the heat removed by the chips [32].

It was observed that both the average and maximum temperatures show a steady increase with the cutting length. This could be explained based on the SEM images and the wear measurements, which confirm that flank wear of carbide tools is relatively higher compared to PCD tools. This will deteriorate the sharp tip of the tool, facilitates wear and rubbing friction, subsequently increasing the temperature.

By comparing the cutting conditions R2 with R6 and R4 with R8, which explains the effect of depth of cut, it can be inferred that average and maximum temperature at a depth of cut 2.5 mm is lower than that at a depth of cut of 5 mm. This is because when the depth of cut increases, the size of the chip and friction of chip and tool increases leading to an increase in temperature. Thus, we can conclude that higher values of cut-

ting speed and depth of cut and lower value of feed speed lead to higher average and maximum temperature. The temperature recorded by the IR camera was less than the temperature required for the failure of the tool through the thermal degradation process, which is approximately 1000 °C. Hence it is clear that the tool possesses sufficient strength at elevated temperatures. Though the average and maximum temperature is measured, it is preferred to use average temperature for analysis as the maximum temperature may also include the temperature of chips generated [32, 33].

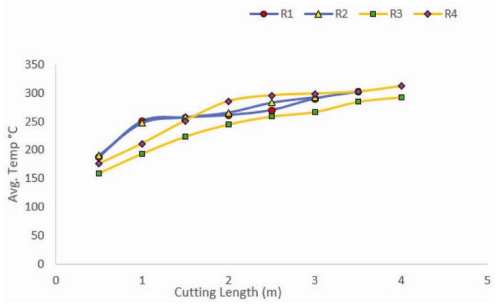

(a)

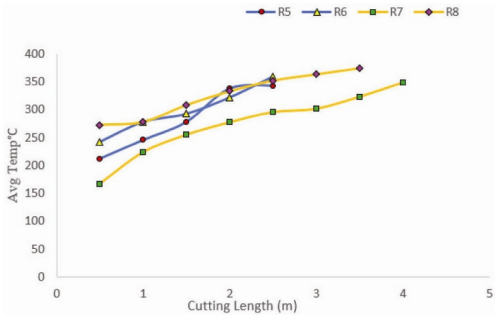

(b)

Fig. 13. Variation of average temperature against cutting length: (a) of R 1, 2, 3, 4; (b) of R 5, 6, 7, 8.

3.5 Cutting forces

The variation of the normal, feed, and axial forces is shown in Figs. 15-17, respectively. The normal force increases with an increase in cutting length, depth of cut, and feed speed and decreases with an increase in cutting speed. At low cutting speeds, the tool ploughs the workpiece leading to high normal forces, whereas, at high cutting speeds, the cutting force becomes steady and subsequently reduces the normal force. It was observed that after an initial rise, feed force decreased in magnitude and gradually attained constancy. This is possibly due to the steady phase of cutting, which reduces the feed force. It was also noted that feed force is dependent primarily on cutting speed and depth of cut and less dependent on feed speed. The tools which showed higher feed force was found to have high values of flank wear, which makes it a good indicator of tool wear. Though very small in magnitude relative to normal and feed forces, the carbide tool also creates an axial force component (F_z), which increases with an increase in feed speed and depth of cut and less dependent on cutting speed. The resultant of the three forces (resultant force) is plotted

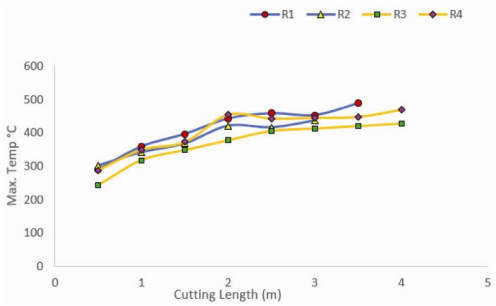

(a)

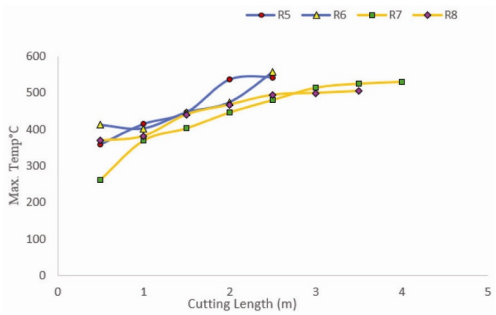

(b)

Fig. 14. Variation of maximum temperature against cutting length: (a) of R 1, 2, 3, 4; (b) of R 5, 6, 7, 8.

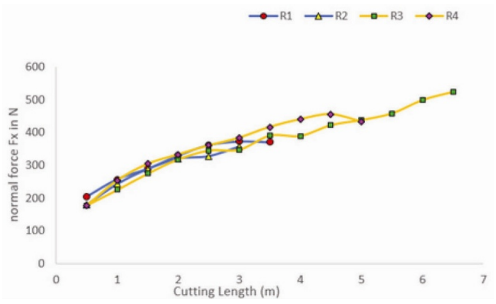

(a)

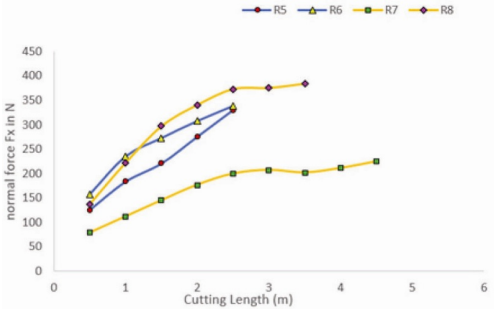

(b)

Fig. 15. Variation of normal forces against cutting length: (a) of R 1, 2, 3, 4; (b) of R 5, 6, 7, 8.

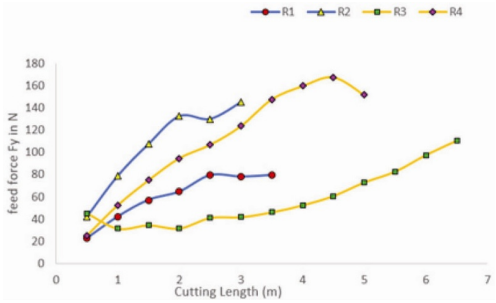

(a)

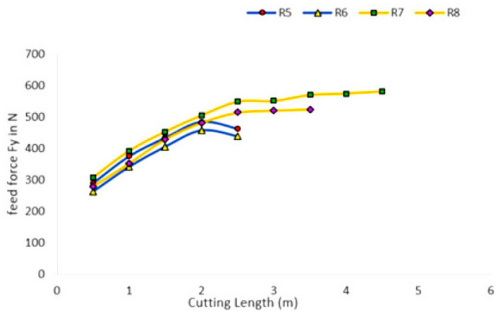

(b)

Fig. 16. Variation of feed forces against cutting length: (a) of R 1, 2, 3, 4; (b) of R 5, 6, 7, 8.

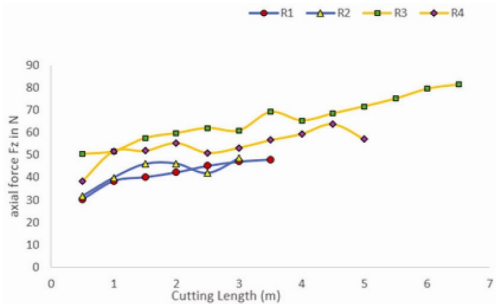

(a)

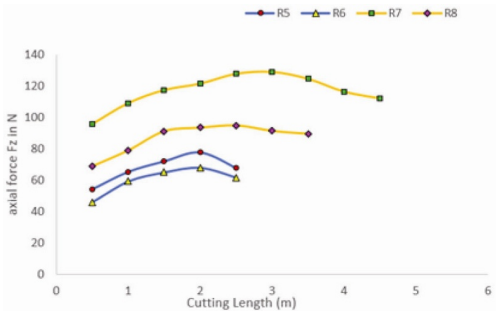

(b)

Fig. 17. Variation of axial forces against cutting length: (a) of R 1, 2, 3, 4; (b) of R 5, 6, 7, 8.

against cutting length as in Fig. 18.

3.6 Power

Power increased with an increase in feed speed and depth

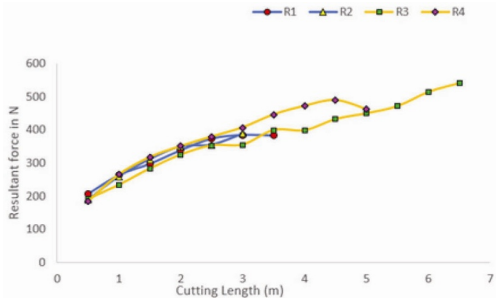

(a)

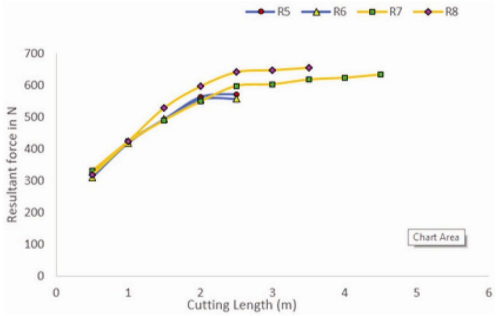

(b)

Fig. 18. Variation of resultant force against cutting length: (a) of R 1, 2, 3, 4; (b) of R 5, 6, 7, 8.

of cut and was less dependent on cutting speed. This is evident from the graph (Fig. 19) as there is only a slight increase in power for the cutting conditions R2 and R6 when compared with R1 and R5, respectively (similar feed, depth of cut but different cutting speed condition). Furthermore, with an increase in cutting length, net power increased in the initial stages and gradually attained constancy. This could be explained based on the relatively high tool wear in the initial passes and the subsequent steady phase of cutting. It can also be noted that power is a good indicator of wear as the power consumption curve during the machining experiments is similar to the wear pattern observed. Justifying this, the tool, when operated under cutting conditions associated with high power (R8), produced maximum flank wear.

3.7 Correlation with tool wear

To determine the correlation between tool wear and different machining responses, a linear regression was conducted to statistically measure the closeness of the data to the regression line. Coefficient of determination (R^2) values were close to one for average temperature, resultant force, and power. The close range of values in linear regression led to the development of a non-linear regression model, which is more conclusive.

A nonlinear regression to establish the relationship between tool wear and different parameters was performed using Sigma plot software for a better understanding of this correlation. The general expression for an expanded tool wear regression model is shown below.

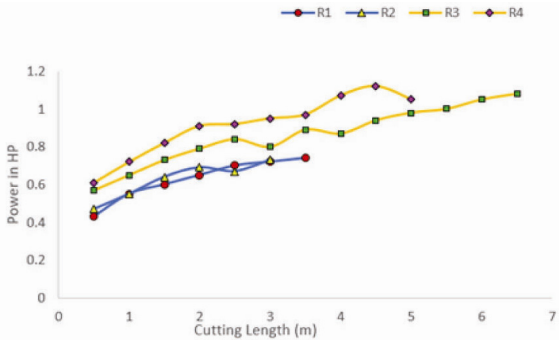

(a)

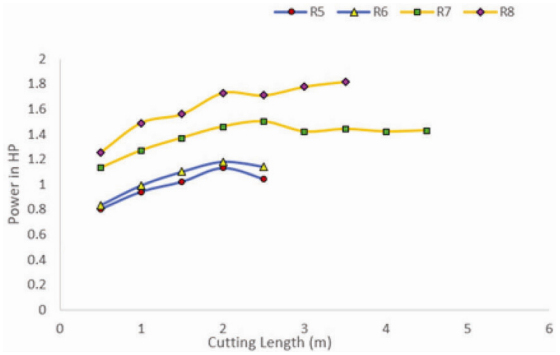

(b)

Fig. 19. Variation of power against cutting length: (a) of R 1, 2, 3, 4; (b) of R 5, 6, 7, 8.

$$T_w = aV^n f^m d^q L^g A^h P^i F^j \quad (2)$$

where a denotes the constant term and n, m, q, g, h, i and j denotes the coefficients of different terms in the tool wear equation. This equation can be used to establish the relationship between tool wear and other parameters. For conducting non-linear regression, parameters that showed a high R^2 value in linear regression were taken. This was performed by taking tool wear along the x axis and the responses along the y axis. A linear regression was conducted to statistically measure the closeness of the data to the regression line. Coefficient of determination (R^2) values was found out for each response - tool wear combination. R^2 measures the adequacy of the fitted model. An R^2 value close to one suggests that the proposed model demonstrates changes of the response data around the mean. From the analysis it was confirmed that average temperature, resultant force, and power have values of R^2 closer to one. Thus, these parameters are capable of accurately predicting the tool wear. Thus different combinations of power, average temperature, and resultant force along with cutting speed, feed speed, depth of cut, and cutting length were tried, and different models were obtained.

For tungsten carbide, different combinations of average temperature (A), resultant force (F), and power (P) along with cutting speed (V), feed speed (f) and cutting length (L), depth of cut (d) were tried and different regression models for tool wear (T_w) were obtained and are summarized below.

Table 5. Statistical summary of different tool wear models.

Eq. no	R	R^2	Adjust R^2	SEE	F-value	P-value
(3)	0.987	0.974	0.972	13.1288	430.69	<0.0001
(4)	0.986	0.972	0.971	13.453	511.743	<0.0001
(5)	0.987	0.975	0.973	12.916	445.3204	<0.0001
(6)	0.99	0.981	0.979	11.351	483.387	<0.0001

$$T_w = 4.717 f^{-0.454} V^{0.456} L^{0.779} d^{0.5595} P^{-0.2446}, \quad (3)$$

$$T_w = f^{-0.5} V^{0.2873} L^{0.5394} d^{0.178} A^{-0.7557}, \quad (4)$$

$$T_w = f^{-0.357} V^{0.338} L^{0.561} d^{0.384} P^{-0.332} A^{0.92}, \quad (5)$$

$$T_w = f^{-0.301} V^{0.526} L^{0.474} d^{0.432} F^{0.415} A^{0.572} P^{-0.391}. \quad (6)$$

The correlation coefficient (R), coefficient of determination (R^2), standard error of estimate (SEE), P-value and F-value for different models are discussed in Table 5.

R^2 and adjust R^2 for all the models are between 0.986 to 0.99 and 0.972 to 0.981, respectively**.** Thus, the proposed regression models explain approximately 98 % variance in tool wear. The low value of SEE cites less variation of the regression model from the experimental data. All the regression reports have a P-value less than 0.0001. This shows that the predictors used in the model are significant and can be used to estimate tool wear. The F-values are of the range 430 to 511, which suggests good prediction.

The tool life Eq. (6) with feed speed, cutting speed, depth of cut, length of cut, power, average temperature, and resultant force showed a very high R, R^2, and adjust R^2 values of 0.99, 0.98, and 0.979, respectively. Furthermore, it has a high F-value and relatively small T-value. This confirms that after adding power, average temperature and resultant force as an independent variable in the tool wear model, the tool life equation is significantly improved, and the tool wear prediction exceeds that of the Taylors model. Altogether, these equations permit edge trimming of CFRP to be designed such that tool wear is optimized and well forecasted.

To check the adequacy of the model developed using regression with average temperature, power, and resultant force as independent variables, validation tests were conducted by trimming CFRP with tungsten carbide tools under three sets of cutting conditions. The feed speed, cutting speed, and depth of cut in each cutting condition are presented in Table 6. The validation parameters were selected so that they are different than the design of experiments (DOE) parameters, but yet fall within the range specified in Table 3.

The experimental tool wear obtained from validation experiments were compared with the tool wear obtained using regression with average temperature, power, and resultant force as independent variables. To deduce the variation of the values so obtained, the mean square error and percentage error was calculated for each trail. Fig. 20 shows the comparison of experimental and regression tool wear for different runs. An approximate average error of 5 % confirms that the experimental

Table 6. Cutting parameters matrix for validation tests.

Cutting condition	Feed speed (mm/min)	Cutting speed (rpm)	Depth of cut (mm)
1	750	5000	3.75
2	750	6400	2.5
3	1000	6400	4

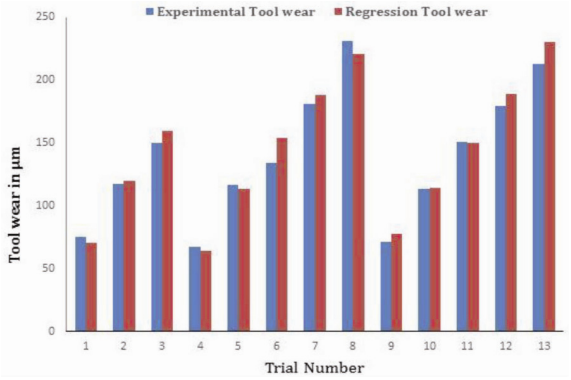

Fig. 20. Comparison of experimental and regression tool wear.

and regression tool wear values are very close. Thus, the regression model adequacy is validated.

4. Conclusions

Experimental studies and further simulations established a clear relationship between the cutting parameters (feed speed, cutting speed, and depth of cut) and response variables (surface roughness, temperature, force, and power). This relationship led to the development of a tool life equation for tungsten carbide tools with respect to cutting speed, feed speed, and depth of cut. Longer tool life was observed at lower values of cutting speed, feed speed, and depth of cut. SEM has allowed discussing the morphologies of the tool during cutting, aiding in developing wear mechanisms. Mathematical modeling of tool wear with a very high degree of accuracy has been developed and validated. The tool life equation with feed speed, cutting speed, depth of cut, length of cut, power, average temperature, and resultant force showed a very high R, R^2, and adjust R^2 values of 0.99, 0.98, and 0.979, respectively. Furthermore, it has a high F-value and relatively small T-value. This confirms that after adding power, average temperature, and resultant force as an independent variable in the tool wear model, the tool life equation is significantly improved, and the tool wear prediction exceeds that of the Taylors model.

One of the limitations of the study is that it is applicable to edge trimming of CFRP using tungsten carbide tools only and not for any other tool-composite combination. The study can be further extended by modelling the temperatures of the tool, workpiece, chip, and heat partition at different cutting feed, speed, and depth of cut. Another area of research could be the application of neural networks to generate real-time tool wear data. In fact, further experimental tests are required by widening the research envelope by adding factors like vibration and dust generated during trimming. A comprehensive predictive model includes the material properties, cutting parameters, response variables, and tool geometry. Additionally, to enhance the accuracy of the model, it is recommended to conduct more trials with different combinations of process parameters.

Acknowledgments

This work is supported by the applied research program of Khalifa University, Abu Dhabi and Strata Manufacturing PJSC, Al Ain, United Arab Emirates.

Nomenclature

f	: Feed rate
V	: Cutting speed
L	: Cutting length
d	: Depth of cut
A	: Average temperature
F	: Resultant force
P	: Power
T_w	: Tool wear
R	: Correlation coefficient
R^2	: Coefficient of determination
SEE	: Standard error of estimate

References

[1] R. Teti, Machining of composite materials, *CIRP Annals-Manufacturing Technology,* 51 (2002) 611-634.

[2] W. König, C. Wulf, P. Grab and H. Willerscheid, Machining of fibre reinforced plastics, *CIRP Annals-Manufacturing Technology,* 34 (1985) 537-548.

[3] Z. Jia, Y. Su, B. Niu, B. Zhang and F. Wang, The interaction between the cutting force and induced sub-surface damage in machining of carbon fiber-reinforced plastics, *Journal of Reinforced Plastics and Composites,* 35 (2016) 712-726.

[4] M. Rahman, S. Ramakrishna and H. C. Thoo, Machinability study of carbon/peek composites, *Machining Science and Technology,* 3 (1999) 49-59.

[5] G. Santhanakrishnan, R. Krishnamurthy and S. K. Malhotra, Machinability characteristics of fibre reinforced plastics composites, *Journal of Mechanical Working Technology,* 17 (1988) 195-204.

[6] Y. Yuefeng, C. Wuyi and G. Liansheng, Tool materials rapid selection based on initial wear, *Chinese Journal of Aeronautics,* 23 (2010) 386-392.

[7] D. Che, I. Saxena, P. Han, P. Guo and K. F. Ehmann, Machining of carbon fiber reinforced plastics/polymers: a literature review, *Journal of Manufacturing Science and Engineering,* 136 (2014) 034001.

[8] K. Sakuma, M. Seto, M. Taniguchi and Y. Yokoo, Tool wear in cutting carbon-fiber-reinforced plastics: the effect of physical properties of tool materials, *Bulletin of JSME,* 28 (1985) 2781-2788.

[9] J. Y. Sheikh-Ahmad and T. Morita, Tool coatings for wood machining: problems and prospects, *Forest Products Journal,* 52 (2002) 43.
[10] A. Sadat, Delamination and other types of damage of graphite/epoxy composite caused by machining, *Joint Applied Mechanics and Materials Summer Meeting*, Los Angeles (1995).
[11] T. Furuki, T. Hirogaki and E. Aoyama, Influence of tool shape and coating type on machined surface quality in face milling of CFRP, *Advanced Materials Research,* 1017 (2014) 310-315.
[12] A. Koplev, A. Lystrup and T. Vorm, The cutting process, chips, and cutting forces in machining CFRP, *Composites*, 4 (1983) 371-376.
[13] G. Santhanakrishnan, R. Krishnamurthy and S. K. Malhotra, Mechanics of tool wear during machining of advanced fibrous composites, *Machining of Advanced Materials* (1993) 489-500.
[14] P. S. Sreejith, R. Krishnamurthy, S. K. Malhotra and K. Narayanasamy, Evaluation of PCD tool performance during machining of carbon/phenolic ablative composites, *Journal of Materials Processing Technology*, 104 (2000) 53-58.
[15] M. Ucar and Y. Wang, End-milling machinability of a carbon fiber reinforced laminated composite, *Journal of Advanced Materials*, 37 (2005) 46-52.
[16] Z. Jia, Y. Su, B. Niu, Y. Bai and G. Bi, Deterioration of polycrystalline diamond tools in milling of carbon-fiber-reinforced plastic, *Journal of Composite Materials*, 51 (16) (2016) 2277-2290.
[17] P. Janardhan, J. Sheikh-Ahmad and H. Cheraghi, Edge trimming of CFRP with diamond interlocking tools, *Proceedings of Aerospace Manufacturing and Automated Fastening Conference*, Toulouse (2006).
[18] J. Sheikh-Ahmad and J. A. Bailey, The wear characteristics of some cemented tungsten carbides in machining particleboard, *Wear,* 225-229 (4) (1999) 256-266.
[19] N. K. Muhamad Khairussaleh, C. H. Che Haron and J. A. Ghani, Study on wear mechanism of solid carbide cutting tool in milling CFRP, *Journal of Materials Research*, 31 (2016) 1893-1899.
[20] M. Haddad, R. Zitoune, F. Eyma and B. Castanie, Study of the surface defects and dust generated during trimming of CFRP: influence of tool geometry, machining parameters and cutting speed range, *Composites Part A: Applied Science and Manufacturing,* 66 (2014) 142-154.
[21] R. Prakash, V. Krishnaraj, G. Tarun, M. Vijayagopal and G. D. Kumar, Experimental study on temperature effect and tool wear on edge trimming of carbon fiber reinforced plastics, *Applied Mechanics and Materials* (2014) 333-338.
[22] M. Slamani, J.-F. Chatelain and H. Hamedanianpour, Comparison of two models for predicting tool wear and cutting force components during high speed trimming of CFRP, *International Journal of Material Forming,* 8 (2015) 305-316.
[23] J. Sheikh-Ahmad, *Machining of Polymer Composites*, Springer, New York (2009).
[24] Y. Takeshi, O. Takayuki and S. Hiroyuki, Temperature measurement of cutting tool and machined surface layer in milling of CFRP, *International Journal of Machine Tools and Manufacture,* 70 (7) (2013) 63-69.
[25] K. Weinert and C. Kempmann, Cutting temperatures and their effects on the machining behaviour in drilling reinforced plastic composites, *Advanced Engineering Materials,* 6 (2004) 684-689.
[26] W. C. Chen, Some experimental investigations in the drilling of carbon fiber-reinforced plastic (CFRP) composite laminates, *International Journal of Machine Tools and Manufacture,* 37 (1997) 1097-1108.
[27] P. Janardhan, Tool wear of diamond interlocked tools in routing of CFRP composites, *M.S. Thesis*, Wichita State University, USA (2005).
[28] M. Slamani, J.-F. Chatelain and H. Hamedanianpour, Comparison of two models for predicting tool wear and cutting force components during high speed trimming of CFRP, *International Journal of Material Forming,* 8 (2015) 305-316.
[29] I. Zaghbani, J. F. Chatelain, V. Songmene, S. Bérubé and A. Atarsia, A comprehensive analysis of cutting forces during routing of multilayer carbon fiber-reinforced polymer laminates, *Journal of Composite Materials,* 46 (2012) 1955-1971.
[30] J. L. Mercy, S. Prakash, A. Krishnamoorthy, S. Ramesh and D. A. Anand, Experimental investigation and multiresponse genetic optimization of drilling parameters for self-healing GFRP, *Journal of Mechanical Science and Technology*, 31 (2017) 3777-3785.
[31] S. Prakash, J. L. Mercy, K. Palanikumar, S. Ramesh, M. I. Rizwan Jamal and A. J. Michael, Experimental studies on surface roughness in drilling MDF composite panels using taguchi and regression analysis method, *Journal of Applied Sciences*, 12 (2012) 978-984.
[32] J. Sheikh-Ahmad, F. Almaskari and F. Hafeez, Heat partition in edge trimming of fiber reinforced polymer composites, *Journal of Composite Materials*, 54 (2020) 2805-2821.
[33] J. Sheikh-Ahmad, F. Almaskari and F. Hafeez, Thermal aspects in machining CFRPs: effect of cutter type and cutting parameters, *The International Journal of Advanced Manufacturing Technology* (2019) 2569-2582.

Deviprakash Jyothi Devan is a Ph.D. student at the Oklahoma State University, United States. He completed his Master's degree from Khalifa University, Abu Dhabi, UAE and Bachelor's degree from Kerala University, India. All his majors are in Mechanical Engineering. His research interest is in composite machining, electromechanical and surface characterization, energy storage devices and batteries.

Fahad Almaskari is an Assistant Professor in the Department of Aerospace Engineering, Khalifa University, Abu Dhabi. He received a Ph.D. in Mechanical Engineering from University of Manchester, UK. His specialization is in solid mechanics and his research interests include modeling and testing of composite materials.

Jamal Sheikh-Ahmad is a Professor in the Department of Mechanical Engineering, Khalifa University, Abu Dhabi. He received a Ph.D. in Mechanical Engineering from North Carolina State University, United States in 1993. His research focuses in the areas of machining polymer composites, friction stir welding and energy efficiency, metal machining by both traditional and nontraditional techniques.

Farrukh Hafeez is a Lecturer in the Department of Mechanical Engineering in the School of Engineering, University of Birmingham, Dubai. He received a Ph.D. in Mechanical Engineering from University of Manchester, UK in 2010. His research interest is in mechanics, machining, and damage of composites.